Minnesota Department of Transportation

RESEARCH SERVICES & LIBRARY

Office of Transportation System Management

Estimating the Crash Reduction and Vehicle Dynamics Effects of Flashing LED Stop Signs

Gary A. Davis, Principal Investigator
Department of Civil Engineering
University of Minnesota

January 2014

Research Project
Final Report 2014-02

LRRB
LOCAL ROAD RESEARCH BOARD

To request this document in an alternative format call 651-366-4718 or 1-800-657-3774 (Greater Minnesota) or email your request to ADArequest.dot@state.mn.us. Please request at least one week in advance.

Technical Report Documentation Page

1. Report No.	2.	3. Recipients Accession No.
2014-02		

4. Title and Subtitle	5. Report Date
Estimating the Crash Reduction and Vehicle Dynamics Effects of Flashing LED Stop Signs	January 2014
	6.

7. Author(s)	8. Performing Organization Report No.
Gary A. Davis, John Hourdos, Hui Xiong	

9. Performing Organization Name and Address	10. Project/Task/Work Unit No.
Department of Civil Engineering University of Minnesota 500 Pillsbury Drive SE Minneapolis, MN 55455	CTS Project # 2011003
	11. Contract (C) or Grant (G) No. (C) 89261 (WO) 195

12. Sponsoring Organization Name and Address	13. Type of Report and Period Covered
Minnesota Department of Transportation Research Services & Library 395 John Ireland Boulevard, MS 330 St. Paul, MN 55155	Final Report
	14. Sponsoring Agency Code

15. Supplementary Notes

http://www.lrrb.org/pdf/201402.pdf

16. Abstract (Limit: 250 words)

A flashing LED stop sign is essentially a normal octagonal stop sign with light emitted diodes (LED) on the stop sign's corners. A hierarchical Bayes observational before/after study found an estimated reduction of about 41.5% in right-angle crashes, but with 95% confidence this reduction could be anywhere between 0% and 70.8%. In a field study, portable video equipment was used to record vehicle approaches at an intersection before and after installation of flashing LED stop signs. After installing the flashing stop signs, there was no change in the relative proportion of clear stops to clear non-stops when minor approach drivers did not face opposing traffic, but the relative proportion of clear stops increased for drivers who did encounter opposing traffic. Random samples of 60 minor approach vehicles were selected before and after installation of flashing LED stop signs and speeds for these vehicles when about 500 feet from the intersection, and average deceleration rates over the final 500 feet, were estimated using trajectory-based methods. Average approach speeds tended to be highest in June, somewhat lower in July, and lower yet in September and November, with September and November having roughly equal average speeds. The average deceleration rates showed a similar pattern.

17. Document Analysis/Descriptors	18. Availability Statement
Stop Signs, Flashing traffic signals, Crash modification factor, Crash causes, Driver performance	No restrictions. Document available from: National Technical Information Services, Alexandria, Virginia 22312

19. Security Class (this report)	20. Security Class (this page)	21. No. of Pages	22. Price
Unclassified	Unclassified	52	

Estimating the Crash Reduction and Vehicle Dynamics Effects of Flashing LED Stop Signs

Final Report

Prepared by:

Gary A. Davis
John Hourdos
Hui Xiong
Department of Civil Engineering
University of Minnesota

January 2014

Published by:

Minnesota Department of Transportation
Research Services & Library
395 John Ireland Boulevard, MS 330
St. Paul, Minnesota 55155

Acknowledgements

The authors would like to thank Chen-Fu Liao, Ted Morris, and Stephen Zitzow of the Minnesota Traffic Observatory for collecting the field video data. University of Minnesota undergraduate student Thomas Hall and graduate student Ning Zhang performed much of the reduction of the field data. From MnDOT, Brad Estochen and Nathan Drews provided intersection and crash data used in the statistical study and Shirlee Sherkow provided administrative support.

Table of Contents

List of Figures

List of Tables

Executive Summary

A flashing LED stop sign is essentially a normal octagonal stop sign with light emitted diodes (LED) on the stop sign's corners. The hope is that the LEDs will increase the conspicuity of the stop sign and reduce the frequency of angle crashes at stop-controlled intersections. In 2009, a Minnesota Department of Transportation (MnDOT) Research Needs Statement indicated:

> "Traffic engineers have installed flashing lights on stop signs in an attempt to improve safety at these intersections. Research is needed to determine if these installations had a positive impact on safety."

In response to this statement, researchers associated with the Minnesota Traffic Observatory at the University of Minnesota conducted a two-pronged investigation of the safety-related effects of flashing LED stop signs: a statistical study to estimate the crash reduction effect following installation of flashing LED stop signs and a field study looking at changes in the behavior of drivers approaching a stop-controlled intersection, before and after installation of a flashing LED stop sign.

The statistical study focused on the effect of installing flashing LED stop signs at through-stop controlled intersections with undivided major roads. The target crash type was right-angle crashes involving major approach and minor approach vehicles. The study design was an observational before/after study, where a reference group of untreated intersections was used to develop a statistical model for predicting the crash experience without the flashing LED stop signs. A treatment group of intersections, where the flashing LED stop signs have been installed was also identified, and the after installation crash experience was compared to the predicted crash experience to estimate the cash reduction effect. A survey of MnDOT district and Minnesota County engineers identified intersections where flashing LED stop signs had been installed, of which 15 had at least three years' worth of after-installation crash data available by 2012. The reference group of intersections was constructed by identifying stop-controlled intersections on trunk highways within 20 miles of one the flashing LED intersections. The estimated reduction was about 41.5%, but with 95% confidence this reduction could be anywhere between 0% and 70.8%. The conclusion was that installation of the flashing LED stop signs reduced the frequency of angle crashes but that the magnitude of this reduction was uncertain.

For the field study, an intersection of a two-lane state highway and a two-lane county highway in Chisago County was selected, with standard stop signs on the county highway. During two, three-day periods in June and July 2012, portable video equipment was used to record vehicle approaches at this intersection, and then the standard stop signs were replaced with flashing LED stop signs. Video data were then collected for two, three-day periods in September and November 2012. Visual inspection of the video was then done to classify each approach vehicle as "clearly stopped" if it appeared to achieve zero-speed before continuing into the intersection, "clearly not stopped" if it appeared to have non-zero speed throughout its maneuver, and "unclear" if it was not possible to decide between "clear stop" and "clear non-stop." Arguably the most interesting result from this analysis was that, after installing the flashing stop sign, there was no change in the relative proportion of clear stops to clear non-stops when minor approach drivers did not face opposing traffic, but that after installation of the

flashing LED stop sign the relative proportion of clear stops increased for drivers who did encounter opposing traffic.

In addition, for each of the four field data collection periods, a random sample of 30 minor approach vehicles was selected. Speeds for these vehicles, when about 500 feet from the intersection, and average deceleration rates over the final 500 feet, were then estimated using trajectory-based methods. Average approach speeds tended to be highest in June, somewhat lower in July, and lower yet in September and November, with September and November having roughly equal average speeds. The average deceleration rates showed a similar pattern.

Chapter 1
Introduction and Literature Review

1.1 Background

A flashing LED stop sign is essentially a normal octagonal stop sign with light emitted diodes (LED) on the stop sign's corners. The hope is that the LEDs will increase the conspicuity of the stop sign and reduce the frequency of angle crashes at stop-controlled intersections. In 2009, the Minnesota Dept. of Transportation (MnDOT) Research Needs 027 stated:

> "Traffic engineers have installed flashing lights on stop signs in an attempt to improve safety at these intersections. Research is needed to determine if these installations had a positive impact on safety."

In response to this statement, researchers associated with the Minnesota Traffic Observatory proposed a two-pronged investigation of the safety-related effects of flashing LED stop signs. The structure of this project is depicted in Figure 1.1.

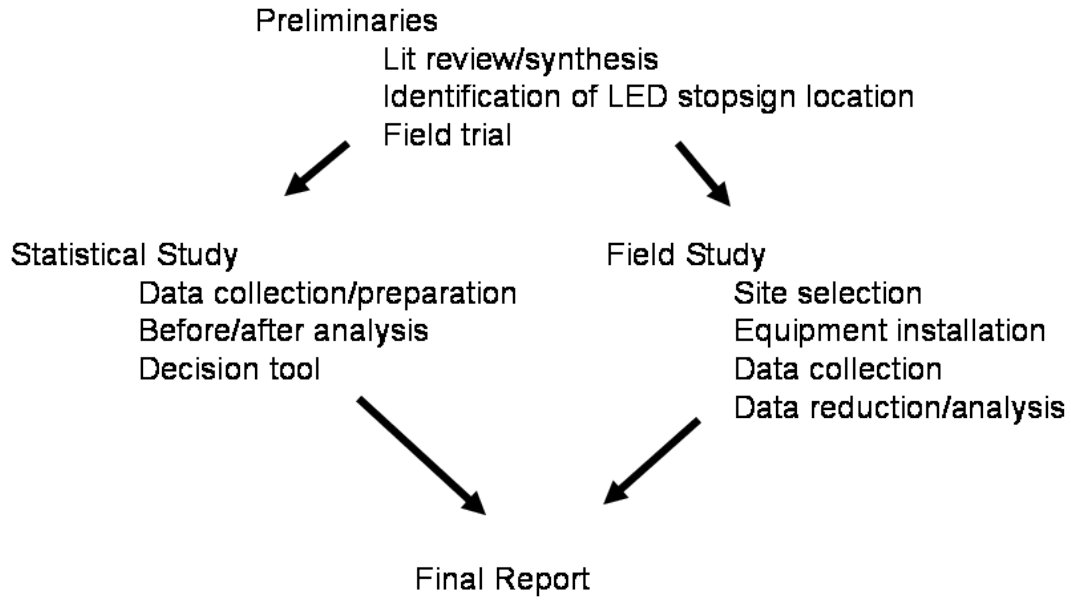

Figure 1.1 Organization of Project

Essentially, this project proposed to make three main contributions to the state of knowledge regarding flashing LED stop signs: a review of literature regarding these and related safety treatments, a before-after study to estimate a crash-modification factor associated with flashing LED stop signs, and a field study of the behavior of individual drivers when approaching an intersection with, and without a flashing LED stop sign. The project also proposed to develop a spreadsheet-based tool to assist engineers in deciding whether or not to install flashing LED stop signs at a given intersection. Chapter 2 of this report describes the before-after study, while Chapter 3 describes the conduct and outcome of the field study. Chapter 4 then describes the decision support tool, based on the results from the before-after study. The remainder of Chapter 1 describes the review of literature.

1.2 Literature Review

As of this date, there does not appear to be any well-conducted research attempting to estimate the crash reduction effects of LED-equipped stop signs. This review was therefore broadened somewhat to include related research dealing with the following configurations:

Pole or pedestal-mounted beacons above a stop sign
Overhead beacons above the intersections roadway
Stop signs with LEDs on their periphery

The review also includes studies of safety-related behavior (e.g. approach speed, stopping compliance) in addition to estimation of crash reductions.

1.2.1 Warning Flashers at Rural Intersections, Stirling Stackhouse and Paul Cassidy, Minnesota Dept. of Transportation, St., Paul, MN, 1998.

This report presented results from a study commissioned by the MnDOT and conducted by the Human Factors Research Laboratory at the University of Minnesota, between 1995 and 1997.

The focus of this investigation was rural, two-way stop-controlled intersections with three types of salience-enhancing installations:

pedestal-mounted flashing yellow beacons on advance-warning (intersection-ahead) signs
pedestal-mounted flashing red beacons above stop signs
overhead beacons showing flashing red to minor (stop-controlled) approaches and yellow to major approaches.

The project reported four separate activities relevant to its objective: a literature review, an opinion survey of drivers, a before-after study, and a field study.

Literature review: The authors reviewed a wide range of literature falling into five general categories: (1) lighting at rural intersections, (2) pavement markings and rumble strips at rural intersections, (3) sight distance and visual field at intersections, (4) traffic signals at rural intersections, (5) traffic signs at rural intersections. The authors concluded that little of this literature was directly relevant to the focus of the project, and that inconsistent results were found when comparing different reports.

Opinion Survey: A mail survey with questions regarding use of flashing lights at rural intersections was returned by 144 drivers. The authors concluded that while drivers tended to interpret flashing lights as indicating an intersection that was more dangerous than one without lights, the findings did not show that drivers tended to reduce speeds because of the lights. They also reported a tendency to interpret the overhead flashing red beacon as indicating a four-way stop, i.e. one where major approach drivers would be expected to stop as well.

Before/After Study: The authors identified 12 rural, two-way, stop-controlled intersections where three years' worth of crash data were available before and after the installation of flashing lights. For eight intersections that were switched from no flashers to overhead flashers, the authors reported, on average, a 39% reduction in crashes. For four intersections which went from no flashers to pedestal-mounted flashers the authors reported a 40% reduction in crashes. Control for possible regression-to-mean effects was not done, and tests for statistical significance of effects were not reported.

Field study: A field study of driver behavior before and after installation of flashing indications was conducted at the intersection of USTH 14 and MNTH 42/CSAH 7, in Olmstead County. The MNTH42 and CSAH 7 approaches were stop-controlled. Driver speeds were measured by pavement-based magnetic sensors on both major and minor approaches. Originally,

a complete experiment of different combinations of flasher configurations was planned, but vandalism, theft, and sensor failures limited the comparisons that could be made. In particular, only data for the baseline (no flashers) condition was available for the minor road approach. The authors concluded that the overhead flashers did not have significant effect on major-approach speeds.

Despite the rather dramatic decrease in crash experience, the authors concluded that their study did not provide unequivocal evidence for safety benefits of overhead flashers. In part this could be due to the inability of results from the field study to confirm the results from the crash analysis.

1.2.2. "Development of Crash Reduction Factors for Overhead Flashing Beacons at Rural Intersections in North Carolina," Brian Murphy and Joseph Hummer, Transportation Research Record, 2030, 2007, 15-21.

This study focused on rural intersections of two two-lane roads, with no turn lanes, and two-way stop control. The treatment was the installation of overhead beacons, with flashing yellow on major approaches and flashing red on stop-controlled approaches.

The authors identified 34 North Carolina intersections where the target configuration had been installed, and where at least three years of post-installation crash data were available. Because the target configuration is used in North Carolina at intersections showing atypical crash experience, the authors felt that an empirical Bayes before/after method was needed to control for possible regression-to-mean effects. For each of the 34 treatment intersections, five non-treated intersections were chosen to comprise the reference group. After also controlling for the effects of change in traffic volumes, the authors reported a 12% decrease in all crashes, a 9% decrease in injury crashes, a 40% decrease in severe injury crashes, a 9% decrease in frontal impact crashes, and a 26% decrease in crashes were the investigating officer indicated "ran stop sign."

The authors noted that overhead beacons were often installed in response to "high-profile, severe injury, 'ran stop sign'" crashes, and that although the beacons appeared to address this type of crash, the relative rarity of these crashes meant that overall crash reduction effects were fairly modest.

1.2.3. Safety Evaluation of Flashing Beacons at STOP-Controlled Intersections, Rhagavan Srinivasan, Daniel Carter, Kimberly Eccles, Bhagwant Persaud, Nancy Leffler, Craig Lyon, and Roya Amjadi. Federal Highway Administration Report FHWA-HRT-08-044, Washington, DC, 2008.

In this study, both rural and urban intersections, with two-way stop-control or with four-way stop control, and either two-lane or four-lane approaches, were used. The treatment configurations considered were overhead beacons, with flashing yellow on main approaches and flashing red on minor approaches, and pole-mounted flashing red beacons above stop signs.

64 stop-controlled intersections were identified from North Carolina and 42 from South Carolina, where flashing beacons had been installed. An empirical Bayes before/after study design was chosen, so reference groups consisting of several hundred additional stop-controlled intersections were also identified. A number of aggregated and disaggregated analyses were performed. The results most relevant to this review were:

(1) considering all intersections, from both states together, flashing beacons led to about a 13.3% reduction in angle crashes, and a 10.2% reduction in injury crashes;

(2) considering two-way stop-controlled intersections from both states, flashing beacons led to about a 12.7% (±9.4%) reduction in crashes;

(3) considering stop-sign mounted flashing beacons from both states, a 58.2% (±32.6%) reduction was observed;

(4) considering overhead beacons from both states, an 11.9%(±10.8%) reduction was observed.

Overall, the results reported here were roughly consistent with those reported by Murphy and Hummer (2007).

1.2.4. Traffic Operational Impacts of Higher-Conspicuity Sign Material, Timothy Gates, H. Gene Hawkins, Susan Chrysler, Paul Carlson, Andrew Holick and Clifford Spiegelman, Report FHWA/TX-04/4271-1, Federal Highway Administration, Washington, DC, 2003. (a summary of this work is also given in "Field Evaluation of Warning and Regulatory Signs with Enhanced Conspicuity Properties," Transportation Research Record, 1862, 2004, 64-76.)

This field study looked at the driver behavior effects of a range of "higher-conspicuity" treatments: fluorescent yellow chevrons, fluorescent yellow Chevron posts, fluorescent yellow curve signs, fluorescent yellow ramp speed signs, fluorescent yellow stop ahead signs, fluorescent red stop signs, flashing red LED stop signs, and red-bordered speed limit signs. The focus in this review will be on observations related to flashing red LED stop signs.

Two intersections were selected, a suburban intersection with four-way stop control and 35 mph posted speed limit, and a rural intersection with two-way stop control and a 65 mph posted speed limit. The configuration of interest here is a stop sign equipped with flashing LEDs at its corners. Lidar was used to measure vehicle speeds approaching the stop signs, and review of video was used to measure stopping compliance. No analyses using crash data were performed.

No statistically significant changes in mean speed or number of vehicles using decelerations greater than 10 ft/sec^2 were observed at either intersection. At the suburban intersection with 35 mph speed limits, the proportion of vehicles failing to stop declined from 48.5% to 31.7%. At the rural intersection with 65 mph speed limits night-time failure to stop declined from 57.8% to 27.4%, with substantial reductions also occurring for day time and twilight conditions.

1.2.5. Evaluation of Best Practices in Traffic Operations and Safety: Phase I: Flashing LED Stop Signs and Optical Speed Bars, E.D. Arnold and K.E. Lantz, Virginia Transportation Research Council Report VTRC 07-R34, Virginia Transportation Research Council, Charlottesville, VA, 2007.

One T-intersection with one stop-controlled minor approach was chosen. This intersection had experienced 14 reported crashes between 2003 and 2005, with failure to stop being cited for four of these. Driver behavior data were collected before and after installation of a stop sign equipped with flashing LEDs at its corners.

Portable traffic counters were placed approximately 1400 feet, 710 feet, and 375 feet from the stop sign. Before data were collected over a 7-day period. Two sets of after data were collected over 7-day periods, one within one week of installation of the flashing LED sign and one after 90 days. Stopping compliance was measured by field observers, making observations over 7-day periods during the morning peak, the lunch period, the afternoon peak, and evening

periods. Drivers were classified as making voluntary full stops, full stops due to conflicting traffic, rolling stops, and "blowing through" the intersection. No analyses using crash data were conducted.

Decreases in average vehicle speed were observed in the range of 1.3 mph to 3.4 mph. Changes in the personnel available to the stopping compliance study led to inconsistencies that the researchers felt compromised these results.

1.2.6 Summary of Literature Review

Based on two EB before-after studies from the North and South Carolina, it appears that overhead flashing beacons installed at two-way stop-controlled intersections can reduce intersection-related crashes by approximately 12%. An estimate of the reduction effect of angle crashes for pole-mounted beacons on stop signs was approximately 58%, but this had a wide confidence interval (approximately ±33%). A study in Texas of two two-way stop controlled intersections found a substantial change in stopping compliance after LED-equipped stop signs were installed, but little evidence for changes in approach speeds. A study of one, two-way stop-controlled intersection in Virginia reported speed reductions in the range of 1.3-3.4 mph.

Chapter 2
Statistical Estimation of Crash Modification Factor

2.1 Background

As noted in Chapter 1, a flashing LED stop sign is a regular octagonal stop sign with flashing light-emitting diodes on its vertices. The hope is that by increasing the conspicuity of the stop sign the frequency of violations, and related intersection crashes, will be reduced. At present however there does not appear to be conclusive evidence regarding the crash reduction effects of this treatment. The chapter describes an effort to estimate a crash modification factor (CMF) associated with installation of flashing LED stop signs.

The *Highway Safety Manual* (HSM) (AASHTO 2010) defines a crash modification factor as the ratio of the expected crash frequency when the countermeasure is in place to the expected crash frequency without the countermeasure.

$$CMF = \frac{E[N_{with}]}{E[N_{without}]} \tag{2.1}$$

Related to the CMF is what the HSM calls the safety effectiveness (SE) of a countermeasure.

$$SE = 1 - CMF \tag{2.2}$$

When CMF < 1.0, so that the countermeasure appears to have reduced crash frequency, the safety effectiveness can be interpreted as the fraction of crashes prevented.

One might expect that the CMF associated with a safety countermeasure could be estimated by identifying locations where the countermeasure had been implemented and then comparing crash experience before and after implementation. An important methodological concern which should be born in mind is that if a treatment is applied to intersections in response to atypical crash occurrences, then estimates of safety effects computed from standard before-after comparisons will probably be compromised by regression-to-the-mean (RTM) bias. A simple example of RTM occurs when one gets a six after tossing a six-sided die. The probability of getting something less than a six on the next toss is 5/6, even though there is no change in the physical process producing these outcomes. In a similar manner, an intersection which has had a randomly high number of crashes in one year will probably have fewer crashes the next, even if nothing about the intersection has changed. Since the 1980's the potential for RTM to bias estimates of crash modification effects has become well-understood, and Hauer and his associates (Hauer 1997) have developed a set of statistical procedures, based on the empirical Bayes (EB) methodology (Robbins 1956) and described in Chapter 9 of the HSM, to account for this bias. The EB approach starts with a safety performance function (SPF), which is a generalized linear model describing how crash experience at locations without the countermeasure typically varies with respect to a set of site-specific features, such as traffic volumes. The SPF is then used to predict what the crash frequency would have been at a set of locations where a countermeasure has been implemented, had the countermeasure not been applied. This predicted frequency is then compared to the observed after-treatment crash frequency to estimate the crash modification factor. At least under some conditions, this approach leads to consistent (i.e. asymptotically unbiased) estimates of a CMF (Davis 2000a).

One potential weakness to the HSM's EB methodology is that it treats the parameters of the SPF as if they were known with certainty, rather than as estimated values which are more or less uncertain, and this can lead to underestimating the uncertainty associated with an estimated CMF. This weakness was identified by Christiansen and Morris (1997), who proposed a hierarchical Bayesian approach. Here, one begins with a prior (before data become available) uncertainty regarding quantities of interest, expressed as a probability distribution, and then uses Bayes theorem to compute a posterior (after data become available) update to this distribution. The computations required to compute the updated distribution are non-trivial, and Christiansen and Morris used moment-based approximations to the Bayesian posterior distributions. Davis (2000b) illustrated how hierarchical Bayes estimation of crash rates could be accomplished using Markov Chain Monte Carlo (MCMC) computational methods, while Davis and Yang (2001) illustrated how MCMC could be used to estimate parameters in an SPF. Aul and Davis (2006) used hierarchical Bayes implemented via MCMC to estimate CMFs associated with installation of traffic signals. Under the name "full Bayes" this approach is now seeing increasingly frequent application to the estimation of CMFs (e.g. Lan et al 2009; El-Basyouny and Sayed 2010).

2.2 Data Acquisition and Preparation

The first task was to compile data on right-angle crash history, traffic volumes, and other relevant features for intersections where flashing LED stop signs had been installed (the treatment group), along with similar data for a set of comparable intersections where flashing LED stop signs had not been installed (the reference group). In October 2010, survey letters were sent to eight Minnesota Dept. of Transportation (MnDOT) District Traffic Engineers, and 87 Minnesota County Engineers, requesting the following information: (1) the locations of LED stop sign installations, (2) the periods for which the signs were in operation, and (3) the types of traffic control in effect before installation. A total of 29 LED installations were identified based on survey responses, 18 of these being on highways managed by MnDOT with the remainder on county or municipal roads. MnDOT then provided spreadsheets with summary statistics and location information for approximately 15,000 stop-controlled intersections in Minnesota. Using this information, the route and milepost information for the 18 trunk highway LED stop sign intersections were determined, and a reference group was then defined as all two-way stop-controlled intersections on the same highways, and within 20 miles of one of the treatment group intersections.

In 2011 a request was made to the Highway Safety Information System (HSIS) for crash records, traffic volumes, and roadway features for all through-stop intersections satisfying the specified route number and mile post range conditions, for the years 2002-2009. These data were then supplemented, using the Minnesota Crash Mapping Analysis Tool (MNCMAT), with crash data for the treatment sites for the year 2010, and to add data for county road treatment sites not available in HSIS. All treatment group and reference group sites were then checked using Google Street View and Google Maps. The site-specific information such as the number of legs, whether or not the intersection had skewed approaches, and its traffic control type, were recorded. A total of 11 of reference sites were found to be either signalized, with divided major roads, or to have no stop signs, and were dropped. As they became available, the crash history for the treatment sites was supplemented with crash data from the years 2011 and 2012. This ultimately gave a total of 15 treatment sites with at least three years of data after installation of the flashing LED stop signs, for a total of 59 site-years. The reference group had approximately

240 intersections, with a total of 1884 site-years of reference group data which included before periods for the treatment group intersections.

With the help of District Traffic Engineers, five intersections in the treatment group and three intersections in the reference group were identified as having pole-mounted beacons, and the years in operation for the beacons were obtained as well. A Microsoft Access database was created containing the crash, traffic, and intersection configuration data and using Access it was possible to compile, for each year and each intersection, the counts of right-angle crashes, the average daily entering traffic volumes (ADT) on the major and minor approaches, the speed limits on the major and minor approaches, whether or not an intersection was a four-legged versus a T-intersection, whether or not at least one minor approach was skewed (for both HSIS and Google Maps observations), and whether or not an intersection had pole-mounted beacons installed. Two text files, one containing reference group data (dataset 1), and one containing treatment group data for years after the LED installation (dataset 2), were then prepared.

2.3 Statistical Modeling

In the hierarchical Bayesian approach to estimating the CMF for flashing LED stop signs, the observed right-angle crash frequency at intersection *k* during year *t* is modeled as a Poisson random variable, with a mean value related to the intersection's characteristics via a random effects generalized linear model (GLM):

$$\mu_{kt} = \mu_{k0}\bar{\mu}_{kt} = \mu_{k0}\exp\left(\beta_0 + \beta_1 X_{kt,1} + \cdots + \beta_m X_{kt,m}\right) \quad (2.3)$$

where μ_{kt} = expected right-angle crash frequency for intersection *k* in year *t*;

μ_{k0} = a site-specific random effect (reflecting effects of unobserved site features);

$\bar{\mu}_{kt}$ = expected right-angle crash frequency for "typical" sites with covariate values $X_{kt,1}$, ... , $X_{kt,m}$;

$X_{kt,j}$ = value of covariable *j*; and

β_0 , …,β_m = GLM coefficients.

Using the reference group dataset, the GLM coefficients and μ_{k0} were estimated first. Then the predicted crash frequency at the treatment intersections, for each treatment year, was calculated using Eq. (2.3) and covariable values appropriate for the given years. This gave predicted crash frequencies for the post-treatment years, had the flashing LED stop signs not been installed. The posterior distribution for the CMF was then simulated as that for a gamma random variable, with an expected (mean) value approximately equal to

$$E[CMF] = \frac{B}{A} \quad (2.4)$$

where

B = total predicted right-angle crash frequencies had the flashing LED stop signs not been installed, i.e. sum of the predicted right-angle crash frequencies over treatment sites and years, and

A = total actual after-installation crashes of treatment sites.

Three models, with different covariates as summarized in Table 2.1, were considered. Model III contained the five common covariates: (1) the logarithm of major approach ADT, (2)

the logarithm of minor approach ADT, (3) a dummy variable indicating whether or not the major approach speed limit was at least 55 mph, (4) a dummy variable indicating whether or not the minor approach speed limit was at least 55 mph and (5) a dummy variable indicating whether or not the intersection was four-legged. In addition to these, Model I included a dummy variable for intersection skewness as determined from the HSIS and a dummy variable for beacon installation. Model II included two dummy variables to represent the discrepancy in intersection skewness as recorded in the HSIS data and as observed using Google Maps.

Table 2.1 Crash Frequency Model Covariate List

Covariate	Description	Used in
X_1	logarithm of major approach ADT	Models I, II, and III
X_2	logarithm of minor approach ADT	
X_3	= 1, if major approach speed limit is greater than or equal to 55 mph; = 0, otherwise	
X_4	= 1, if minor approach speed limit is greater than or equal to 55 mph; = 0, otherwise	
X_5	= 1, if intersection is four-legged; = 0, otherwise	
X_6	= 1, if HSIS shows intersection is skewed; = 0, otherwise	Model I
	= 1, if HSIS and Google Maps observation show intersection is skewed; = 0, otherwise	Model II
X_7	= 1, if a beacon is installed; = 0, otherwise	Model I
	= 1, if HSIS and Google Maps observation are not consistent; = 0, otherwise	Model II

2.4 Results

The GLM coefficients and safety performance functions were computed using the Markov Chain Monte Carlo (MCMC) software WinBUGS (Lunn et al. 2000). Each model had a 5,000 "burn-in" period followed by 60,000 updates (a two-chain run for 30,000 iterations). The WinBUGS estimates for Models I, II, and III are given in Tables 2.2-2.4.

In addition to estimates of a parameter's posterior probability density, WinBUGS also provided the posterior probability that a parameter was greater than zero, and these probabilities are displayed in the final columns of Tables 2.2-2.4. Parameters for which the value zero was either in the 10% or 90% tail of its posterior distribution will be called 'significant.' In Model I, β_6 (a skewed intersection based on HSIS data) and β_7 (beacon installation) have posterior probabilities of being greater than zero equal to 0.123 and 0.665 respectively, suggesting that the predictive value of the corresponding covariates was negligible. In Model II, β_6 (skewed intersection based on both HSIS data and Google Maps observations) and β_7 (a questionable skewed intersection) were not significant, indicating that whether an intersection is skewed and the presence of pole-mounted beacons did not have much impact on the right-angle crash frequencies.

Table 2.2 WinBUGS Estimates for Model I

node	mean	sd	2.5-%ile	97.5-%ile	Prob>0
β_0	-3.345	0.359	-4.08	-2.664	0.0000
β_1	0.373	0.215	-0.049	0.792	0.959
β_2	1.132	0.150	0.857	1.442	1.0000
β_3	-2.688	0.879	-4.522	-1.101	0.00005
β_4	2.392	0.853	0.861	4.180	0.9995
β_5	0.608	0.327	-0.030	1.248	0.9690
β_6	-0.445	0.384	-1.185	0.329	0.123
β_7	0.346	0.751	-0.974	1.979	0.665
SE (1-CMF)	0.424	0.184	-0.00007	0.713	0.975

Table 2.3 WinBUGS Estimates for Model II

node	mean	sd	2.5-%ile	97.5-%ile	Prob>0
β_0	-3.375	0.365	-4.083	-2.663	0.0000
β_1	0.416	0.222	-0.026	0.847	0.969
β_2	1.128	0.149	0.851	1.436	1.0000
β_3	-2.618	0.901	-4.576	-1.068	0.00005
β_4	2.397	0.871	0.897	4.276	0.9995
β_5	0.654	0.334	-0.003	1.307	0.976
β_6	-0.486	0.470	-1.392	0.453	0.150
β_7	-0.448	0.393	-1.203	0.332	0.128
SE (1-CMF)	0.435	0.177	0.003	0.715	0.980

Model III contained five basic covariates, which were also included in Models I and II. In these three models, the coefficients β_0 to β_5 were all significant. The β_1 coefficient was associated with how the expected crash frequency varied with the major approach ADT. β_1's point estimates were 0.373, 0.416, and 0.355 for Model's I, II, and III, respectively. The positive sign for this coefficient means that, plausibly, expected angle crash frequency tended to increase as the major approach ADT increased. Angle crashes also tended to increase as the minor approach ADT increased (β_2), if the minor approach speed limit was 55 mph or greater (β_4), and if the intersection was a four-legged as opposed to a T-intersection (β_5). On the other hand, crashes tended to be less frequent when the major approach speed limit was 55 mph or greater (β_3), most likely because intersections where the major approach speed limit was less than 55 mph tended to be in more urbanized areas.

Table 2.4 WinBUGS Estimates for Model III

node	mean	sd	2.5-%ile	97.5-%ile	Prob>0
β_0	-3.295	0.360	-3.994	-2.592	0.0000
β_1	0.357	0.217	-0.072	0.777	0.948
β_2	1.111	0.143	0.838	1.40	1.0000
β_3	-2.731	0.912	-4.644	-1.089	0.0002
β_4	2.366	0.864	0.811	4.172	0.9997
β_5	0.543	0.318	-0.089	1.15	0.956
SE (1-CMF)	0.415	0.185	-0.014	0.706	0.972

The point estimates for the safety effectiveness (SE) were 0.424, 0.435, and 0.415, respectively, for Models I-III suggesting approximately a 42% decrease in right-angle crashes associated with installation of flashing LED stop signs. However, the 95% confidence intervals for the safety effectiveness were

(-.00007, .713)
(.003, .715)
(-.014, .706)

for the three models, respectively, suggesting that the data were consistent with effects ranging from essentially no change, to a 71% decrease. The posterior probabilities of some decrease in crashes of some magnitude were 0.975, 0.980, 0.972, indicating that a decrease in the frequency of right-angle crashes appeared to be associated with installation of flashing LED stop signs, but that the magnitude of this reduction remains somewhat uncertain.

2.5 Estimation Using the HSM Methodology

As a check on the Bayesian computations, the parameters for Model III were estimated using maximum likelihood, and the safety effectiveness then estimated using the procedure described in Appendix 9A of the HSM. These results are summarized in Table 2.5.

Table 2.5 Most Frequent Estimates for Model III

parameter	point estimate	se	-2se	+2se
β_0	-3.674	0.272	-4.22	-3.13
β_1	0.617	0.157	0.304	0.930
β_2	0.994	0.093	0.808	1.181
β_3	-1.852	0.501	-2.854	-0.851
β_4	1.811	0.497	0.818	2.804
β_5	0.902	0.215	0.472	1.332
SE (1-CMF)	0.461	0.166	0.129	0.793

In Table 2.5, the se column gives the estimates' standard errors, while the final two columns give the ±2se ranges. Comparing Table 2.5 to Table 2.4, it can be seen that the point estimates in

Table 2.5 all fall within the 95% confidence intervals given in Table 2.4, and the estimated safety effectiveness is slightly larger but still consistent with that given in Table 2.4.

Chapter 3
Field Study of Driver Behavior

3.1 Preliminary Work

As noted in Chapter 1, this project consisted of two studies, a statistical study aimed at estimating the crash reduction effect of flashing LED stop signs, and a field study comparing the behavior of drivers at a traditional stop sign to that at a flashing LED stop sign. The working hypotheses for the field study were that, at flashing LED stop signs:

(1) the frequency of drivers failing to stop will be lower than at a traditional stop sign,

(2) drivers will tend to approach a flashing LED stop sign at a lower speed, and will tend to decelerate less abruptly, than drivers approaching a traditional stop sign.

A first requirement then was to identify a data collection strategy that supported

(a) classifying a vehicle's approach as to stopping compliance,
(b) estimating speeds as vehicles approach a stop sign, and
(c) estimating the magnitude of the braking deceleration.

The Minnesota Traffic Observatory (MTO) has developed a system for video-based traffic data collection in the field (see Figure 3.1). It has two main components: (1) a 30-foot retractable aluminum pole with a CCD camera installed on the top; (2) a cabinet at the base that contains a digital video recorder and two 12V lead-acid batteries which power the pump that raises the pole, as well as the camera and the digital recorder. When connected to a laptop computer with a controller program, the camera's start and recording time can be set. Davis and Swenson (2006) described a method by which features of a vehicle's motion, such as speed and acceleration, could be estimated from a video recording of the vehicle's path. However, Davis and Swenson used video shot from a fixed position on the roof of a high-rise building, and it was not clear if this technique could be adapted to the lower-elevation views available from the portable equipment. It was decided then to conduct field tests to resolve this issue.

On November 11, 2010, a trial installation of the MTO's pole-mounted video recording equipment was done at the intersection of Main Street (Trunk Highway 19) and 4th Avenue, in New Prague, MN. This intersection is four-way stop-controlled, with Flashing LED stop signs on all approaches, and there was an abundance of existing infrastructure (light and sign standards) to which the MTO equipment could be anchored. Video recordings of vehicles approaching the intersection were made, and the video data were reduced and analyzed using the following procedure:

Figure 3.1 Minnesota Traffic Observatory's Portable Video System

(1) Prior to data collection, real world coordinates for a set of control points were measured using a measuring wheel and marked so as to be visible in the video. Figure 3.2 shows the camera's view at the test intersection and the locations of the control points.

(2) The trajectory of a vehicle with respect to screen coordinates was measured using the software VideoPoint. Figure 3.3 shows an example of a screen trajectory.

(3) Screen coordinates for the control points were also measured using VideoPoint and these, along with the real-world coordinates for the control points, were used to compute the coefficients C[1], C[2], …, C[8] for the equations

$$x_r = \frac{C[1] + C[2]x_s + C[3]y_s}{1 + C[4]x_s + C[5]y_s}$$
$$y_r = \frac{C[6] + C[7]x_s + C[8]y_s}{1 + C[4]x_s + C[5]y_s} \qquad (3.1)$$

which perform the transformation from the screen coordinates (x_s,y_s) to real-world coordinates (x_r,y_r).

(4) Using equations (3.1), a vehicle's screen trajectory was transformed to its real-world trajectory. Figure 3.4 shows a plot of distance traveled versus time for an example vehicle.

The vehicle's real world trajectory was then described using four elements:

v0 = initial speed

a1 = initial acceleration/deceleration rate

t1 = point at which final deceleration began

a2 = final deceleration rate

Bayes estimates for these elements were computed using the software WinBUGS (Lunn et al. 2000), and Figure 3.4 also shows estimates for these elements. For this vehicle, at the start of data collection the driver was traveling at about v0=24.6 feet/second and decelerating at about

a1=2.04 feet/sec^2. At about time t1=2.15 the driver then increased the deceleration to about a2=6.4 feet/sec^2. Based on the test results, it was decided to use MTO's portable equipment to collect data for the field study.

Figure 3.2 Camera View and Control Points for Field Test

Figure 3.3 Screen Trajectory for an Example Vehicle, Measured Using Videopoint

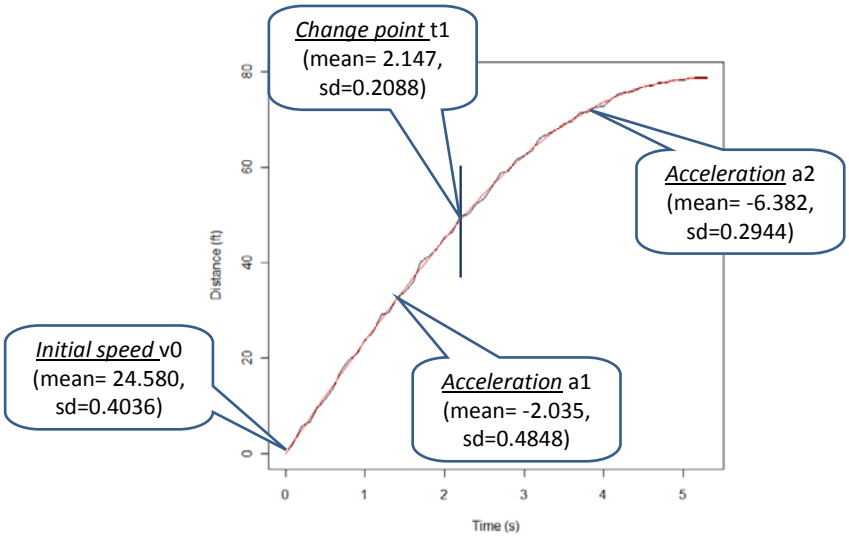

Figure 3.4 Rectified Real-World Trajectory of Example Vehicle and Estimates of Model Elements. Blue Line Denotes Measured Trajectory, Red Line Denotes Trajectory Predicted by Estimated Elements

3.2 Selection of Field Site

The next task was to identify a site or sites at which to conduct the field study. Desirable characteristics of a field site were:

(1) Representative of locations where flashing LED stop signs have/are being considered,

(2) Presence of infrastructure for securing the MTO's video camera and recording equipment,

(3) Within a two-hour drive from the University of Minnesota's Twin Cities campus.

In Spring, 2011 project personnel visited three sites recommended by county engineers, but all were rejected due to lack of mounting infrastructure. Using MNCMAT, project personnel then reviewed two-way stop controlled intersections with non-trivial histories of right-angle crashes, and identified two possible sites:

(1) MNTH 22 & County Rd 8, Blue Earth County

(2) MNTH 22 & County Rd 90, Blue Earth County

These were discussed at the August 2011 TAP meeting, and the County Road 90 site was rejected due to the presence of a flashing beacon. The County Road 8 site was considered plausible, but the presence of tall corn plants and the associated sight distance restriction at that time made current conditions unsuitable for the field study. While waiting for the corn harvest, a third possibility was offered:

(3) MNTH 95 & CSAH 9, Chisago County

Figure 3.5 Anchoring Post and View Looking North at MNTH 95 and Chisago CSAH 9

This site had been reviewed earlier in the study, and rejected because it lacked a secure anchor for video equipment. However, the Chisago County engineer installed an anchoring post on the southeast corner of this intersection and on November 30, 2011 a set of tests were conducted evaluating the suitability of this site with respect to field of view and accuracy of video-based estimates. Video data were collected from 12:40PM-1:20PM. The video data collection device was located at the southeast corner of the intersection, recording south-bound traffic on CSAH 9.

Figure 3.6 Reference Points and Video Camera Field of View, MNTH 95 and CSAH 9

The November 2010 field test had indicated that video-based estimation of vehicle trajectories could be used to estimate features such as speeds and deceleration, but was limited to relatively low-speed approaches. To check on the method's feasibility at higher-speed approaches it was decided to conduct an additional field test at the Chisago County site, with the goal of comparing speeds as estimated from video-based vehicle trajectories to speeds measured with a laser gun. Figure 3.6 shows the camera's view of southbound CSAH 9. 12 reference points were selected, their locations were measured using a measuring wheel and marked on the road. These were marked with paint, and 12 traffic cones were placed on these so they would be visible in the camera's view. The real-world coordinates for the reference points (in ft) were (0, 100) , (0, 200) , (0, 300) , (0, 400) , (0, 500) , (0, 600) , (25.6, 100) , (25.6, 100) , (25.6, 200) , (25.6, 300) , (25.6, 400) , (25.6, 500) , and (25.6, 600). In the video, the farthest two traffic cones ((0, 600) and (25.6, 600)) to the intersection were very difficult to identify thus only the 10 remaining reference points were used in this test. As in the previous field test, VideoPoint was used to obtain screen coordinates for the control points, from a single frame by focusing on the center points of the traffic cones' bottom and recording manually.

When estimating the coefficients for the coordinate transformation equations (3.1) it was important to make the measured control point locations be as close as possible to the real world ones. However due to the video quality constraint, it was difficult to identify their exact locations, especially under the low-light conditions. To improve location accuracy, an iterative model calibration procedure was followed. After recording a set of control point screen coordinates, the point with the largest fitting error was identified from a Leave-One-Out Cross-Validation (LOOCV) scatter plot. Its screen coordinates were re-extracted to replace the old ones. If the new overall fitting errors (SSR, sum-of-squared residual squares) decreased, then the previous point with the second biggest fitting errors was selected and the above procedure was

repeated. However, changing a single point's coordinates can affect all other points and sometimes a decrease on SSR was not archived. If that happened, multiple reference points with highest fitting errors were then selected and their different coordinate combinations were tried. Figure 3.7 shows a scatter plot of the projection model after this calibration.

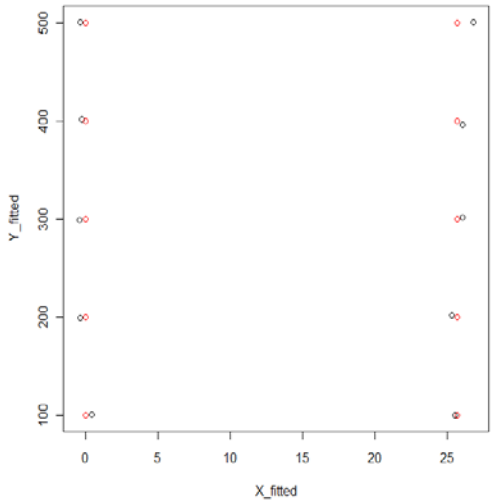

Figure 3.7 Scatter Plot of the Control Point, After Calibration

In the test run, one researcher drove the test vehicle southbound on CSAH 9 while a second used a laser gun to measure range and range rate of the test vehicle at two points along its trajectory:

61.6 feet/sec, at 443feet from the stop bar;

57.2 feet/sec, at 233feet from the stop bar.

As before, the software WinBUGS was used to estimate the elements v0, a1, t1, and a2 describing the vehicle's trajectory, and to make predictions of the vehicle's speed over the course of its trajectory. In order to identify "matched" speeds in WinBUGS output, it was assumed that the distance measured by the laser gun was accurate, and the corresponding estimated speed was then found by matching the estimated distance from WinBUGS with the measured distance.

yr_hat[20]	450.0	0.8382	0.02315	448.4	450.0	451.7	10001	60000
yr_hat[21]	443.8	0.8229	0.02487	442.2	443.8	445.4	10001	60000
yr_hat[22]	437.6	0.8114	0.02645	436.1	437.6	439.2	10001	60000
V[20]	-61.82	0.7079	0.02345	-63.2	-61.82	-60.42	10001	60000
V[21]	-61.86	0.6632	0.02116	-63.16	-61.86	-60.55	10001	60000
V[22]	-61.9	0.6195	0.01888	-63.12	-61.9	-60.68	10001	60000

yr_hat[54]	239.0	0.3116	0.007903	238.4	239.0	239.7	10001	60000
yr_hat[55]	233.2	0.2998	0.007584	232.7	233.2	233.8	10001	60000
yr_hat[56]	227.5	0.2883	0.007271	227.0	227.5	228.1	10001	60000
V[54]	-58.28	0.1266	0.003285	-58.53	-58.28	-58.04	10001	60000
V[55]	-57.51	0.1242	0.003223	-57.76	-57.51	-57.27	10001	60000
V[56]	-56.74	0.1218	0.00316	-56.98	-56.74	-56.51	10001	60000

Figure 3.8 Trajectory-Based Results from Test Run

The trajectory-based estimated computed using WinBUGS are shown in Figure 3.8, where it can be seen that at 443 ft, the closest estimated distance (yr_hat) had time index [21], and corresponding speed V[21] is -61.86ft/s with 95% confidence intervals (-63.16,-60.55). The negative sign for the speeds indicates that the vehicle moving in a direction of decreasing distance from the intersection. The laser gun measured speed 61.6 ft/s falls within this 95% confidence interval. Similarly, at 233ft, the closest estimated distance (yr_hat) had index [55], and the corresponding speed V[55] was -57.51 with 95% CI (-57.76,-57.27). The laser gun measured speed 57.2 ft/s is very close to the 95% upper bound. Taking the laser gun measurement errors into account (±0.5mph), these results indicate that, in this validation test, the trajectory-based model provided reliable speed estimates.

3.3 Field Study Data Collection

On June 7, 2012 MnDOT issued a permit to install the project's data collection equipment at the intersection of MNTH 95 and CSAH 9 in Chisago County, and on June 20, 2012 the anchoring pole for the equipment was re-installed at the site. Data for the before period were then collected on June 26-27 and July 10-12 of 2012. On Sept.14 2012 flashing LED stop signs, denoted by TAPCO, were installed on both approaches of CSAH 9.

Figure 3.9 Flashing LED Stop Sign and Video Equipment on Southeast Corner of Study Site

After-data were then collected on September 17-18, 2012 and November 6-8, 2012. At the start of each data collection period orange cones were placed at the reference locations identified in the field test, to serve as control points for trajectory-based analyses. Several minutes of video were then recorded and the cones were then removed. After allowing for periods when the video was damaged or incomplete, the following numbers of useable approach vehicles were obtained.

Table 3.1 Useable Vehicle Approaches during Each Data Collection Period

Dates	Useable Vehicle Approaches	Hours of Useable Data
6/26-6/27	235	18
7/10-7/12	133	14
9/17-9/18	123	7
11/6-11/8	481	25

The large differences in the numbers of useable events were primarily due gaps in the video record. In addition, a shift in camera position during the September period limited the hours of useable data. For each approach vehicle, a separate video segment was copied from the master recording, and two types of data reduction and analysis were performed.

3.4 Qualitative Analysis of Stopping Compliance

Each vehicle approach was reviewed by a senior undergraduate student, and classified as to vehicle type, movement direction, whether or not the approach vehicle encountered opposing traffic, and the degree of stopping compliance. Stopping compliance was classified as follows:

1: Clearly stopped: approach vehicle appeared to achieve zero speed before turning or proceeding through,

3: Clearly did not stop: approach vehicle appeared to maintain non-zero speed throughout its movement,

2: Unclear: not able to discriminate between 1 and 3.

Each vehicle approach was then reviewed by a graduate student, who gave an independent assessment of degree of stopping compliance. For those approaches where the assessments disagreed, the project's PI provided a third, tie-breaking review. The PI also classified each approach as dark, if only vehicle headlights were visible in the video. Finally, on the afternoon of November 6 a rainstorm occurred, and the PI identified those approaches that were made during rainy/wet-pavement conditions.

Multinomial logistic regression, using the statistical package Minitab, was used to determine if the distribution across the three stopping compliance categories varied with respect to

(1) before versus after installation of the flashing LED stop sign,
(2) whether or not the approach driver was required to yield to opposing traffic,
(3) whether or not the approach occurred at night,
(4) whether or not the approach occurred during rain.

The main goal of the statistical modeling was to determine if, after controlling for weather, lighting, and the presence of opposing traffic, the distribution over the three degrees of stopping compliance was different after installation of the flashing LED stop sign. The weather variable had no statistically significant effect on stopping compliance and was dropped. Figure 3.10 shows results for the final model, which included effects due to whether or not an approaching driver yielded to opposing traffic, whether or not the approach occurred at night, and an interaction effect for yielding after the flashing LED stop sign was installed. The coding of stopping compliance was:

1 = clearly stopped
2 = unclear stop
3 = clearly did not stop

The summary under "Response Information" states that of the 958 useable approaches in the data set, 470 were classified as clearly did not stop, 284 were classified as clearly stopped, and 204 were classified an unclear stop. The tabulation under "Logistic Regression Table" then summarizes how the distribution across the three degrees of stop categories varies with respect to predictor variables. For example, the entries under "Logit 1: (2/3)" compares the relative number of unclear stops to clear non-stops, and the positive coefficient for the predictor "yield01" tells us that vehicle approaches were more likely to be unclear stops when the approaching driver yielded to opposing traffic. The negative coefficient for the "night" predictor tells us that vehicle approaches were less likely to be unclear stops (and so more likely to be clear non-stops) at night.

Response Information

```
Variable  Value       Count
stop      3             470  (Reference Event)
          2             204
          1             284
          Total         958

  958 cases were used
    1 cases contained missing values
```

Logistic Regression Table

```
                                                    Odds         95% CI
Predictor       Coef    SE Coef        Z     P    Ratio    Lower    Upper
Logit 1: (2/3)
Constant    -0.86293    0.09953    -8.67 0.000
yield01       0.8887     0.3669     2.42 0.015     2.43     1.18     4.99
night        -0.7106     0.2397    -2.96 0.003     0.49     0.31     0.79
yxa           0.6972     0.4888     1.43 0.154     2.01     0.77     5.23

Logit 2: (1/3)
Constant     -1.4897     0.1246   -11.96 0.000
yield01       2.9307     0.3042     9.63 0.000    18.74    10.32    34.02
night        -0.6356     0.2696    -2.36 0.018     0.53     0.31     0.90
yxa           0.9193     0.4003     2.30 0.022     2.51     1.14     5.50

Log-likelihood = -810.195
Test that all slopes are zero: G = 370.680, DF = 6, P-Value = 0.000

Goodness-of-Fit Tests

Method      Chi-Square    DF      P
Pearson          3.625     4  0.459
Deviance         4.269     4  0.371
```

Figure 3.10 Nominal Logistic Regression: Stopping Compliance versus yield01, night, yxa

Arguably the most interesting effect is found under "Logit 2: (1/3)," which compares clear stops to clear non-stops. Here, the positive value for the coefficient associated with the predictor "yxa" indicates that there is a statistically significant interaction between the presence of opposing traffic and the period after installation of the flashing LED stop sign. That is, drivers who were required to yield to opposing traffic were more likely to stop, compared non-stop, after the flashing LED stop sign was in place.

To get some idea of the magnitude of this effect, Table 3.2 displays how the estimated odds for clear stop versus clear non-stop varied over the different possibilities during the daytime.

Table 3.2 Odds of Clear Stop vs Clear Non-stop: Daytime

		Flashing LED stop sign	
		Before	After
Opposing Traffic	Absent	0.225	0.225
	Present	4.2	10.6

For example, when opposing traffic was absent:

(Probability of clear stop)/(Probability of clear non-stop) = 0.225,

That is, when opposing traffic was absent there were approximately four clear non-stops for every clear stop, and there was no detectable change in these odds after the flashing LED stop sign was installed. However, when opposing traffic was present there were about 4.2 stops for every non-stop before the flashing LED stop sign was installed, and this ratio increased to about 10.6 stops for every non-stop after the flashing LED stop sign was installed.

In summary, for those approach drivers who did not have to yield to opposing traffic the observed stopping compliance was about the same before and after installation of the flashing LED stop signs. One the other hand, those drivers who did have to yield to opposing traffic were more likely to be seen as clearly stopping after the flashing LED stop sign was installed.

3.5 Analyses of Speed and Deceleration

For each of the four collection periods, 30 approach vehicles were randomly selected for analysis, the only condition being that the vehicles not be traveling in obviously rainy conditions. The approach trajectory for each sampled vehicle was then extracted manually using the program VideoPoint, and the extracted screen trajectories converted to real-world trajectories using the control point locations recorded at the start of the data collection periods. The video quality was such that only the first four control points on each side of the road were discernible and so only these were used to compute real-world trajectories. Since a one-pixel error in determining a vehicle's screen position translates into a much larger real-world error when the vehicle is far from the camera compared to when it is close, two procedures were used to account for this differential measurement error. First, it was decided to restrict analysis to approximately the final 500 feet of the approaches. Second, by computing the derivatives of the transformations given in equation (3.1) it was possible to estimate how a given variance in determining screen position translated into a variance in real-world position error. These real-world variances were used to weight the quality of the real-world positions, with positions closer the camera being given higher weights. Weighted, nonlinear least-squares were then used to estimate four elements describing each vehicle approach:

v0=the initial speed when approximately 500 feet away,
v1=the speed when the driver begins his/her final deceleration,
v2=the speed at the end of the trajectory, and
t1= the time at which the final deceleration began.

From these it was then possible to estimate average deceleration rates for the change from v0 to v2. Figure 3.11 shows the observed and fitted trajectories for one of the vehicles sampled from the June data set.

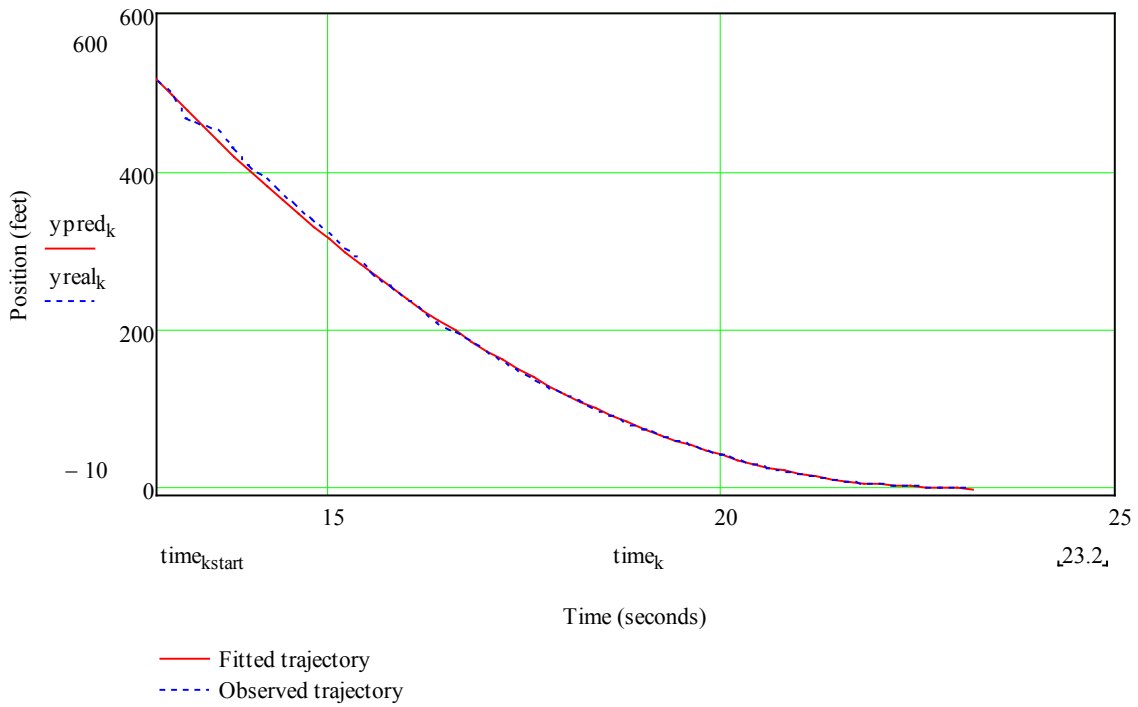

Figure 3.11 Example Observed Trajectory and Fitted Trajectory

Table 3.3 displays summary statistics for the initial speeds (v0) for each of the four data collection periods, while Table 3.4 displays similar information of the average decelerations. Figures 3.12 and 3.13 show graphical summaries of initial speed and average deceleration, respectively.

Table 3.3 Summary Statistics for Vehicle Speeds at 500 feet (miles/hour)

	Average	Standard Deviation	Minimum	Maximum
June	57.6	9.04	37.8	77.2
July	51.2	9.0	36.2	70.4
Sept.	43.6	10.98	17.4	60.0
Nov.	40.6	10.33	23.6	73.5

Table 3.4 Summary Statistics for Average Deceleration (feet/second2)

	Average	Standard Deviation	Minimum	Maximum
June	6.7	2.0	2.9	11.6
July	5.6	1.5	3.4	9.1
Sept.	4.4	1.5	1.1	7.2
Nov.	4.4	1.7	2.0	9.5

Tables 3.3 and 3.4 show similar patterns: higher initial speeds and decelerations in June, somewhat lower speeds and decelerations in July, and yet lower speeds and decelerations in

September and November, with September and November being roughly equal. The average speed at approximately 500 feet from the stop sign was 57 mph in June, 51 mph in July, 43.6 mph in September and 40.6 mph in November. Similarly, average deceleration rates over the final 500 feet of approach went from 6.7 feet/sec^2 in June to 5.6 feet/sec^2 in July, to 4.4 September and 4.4 feet/sec^2 in November.

To summarize, the results displayed in Tables 3.3 and 3.4 suggest a pattern of decreasing speeds and deceleration rates stretching from summer to fall, 2012. The decreases seen between June and July make it difficult to distinguish between an effect due to the flashing LED stop sign and a background trend.

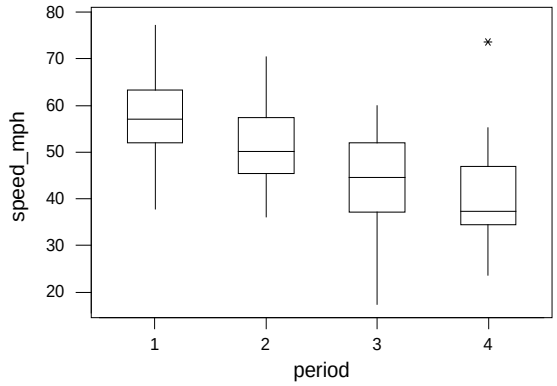

Figure 3.12 Boxplot Summarizing Distributions of Speeds at approximately 500 Feet. 1=June, 2=July, 3=September, 4=November

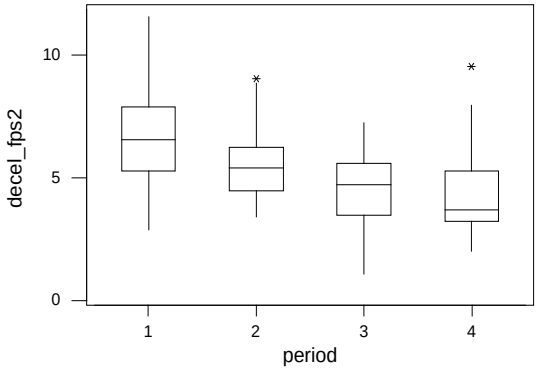

Figure 3.13 Boxplot Summarizing Distributions of Average Decelertion Rates over Final 500 Feet. 1=June, 2=July, 3=September, 4=November

Chapter 4
Decision Support Tool

4.1 Background

The objective of this chapter is to describe a spreadsheet tool, based on the results from Chapter 2, for assisting engineers in deciding where to placed flashing LED stop signs. Imagine that a particular intersection has been proposed for installation of a flashing LED stop sign. Two questions of central importance are:

(1) Are angle crashes a problem at this intersection?
(2) What reduction in angle crashes can be expected if a flashing LED stop sign is installed at this intersection?

As an example, consider the intersection of 160th Street E and County Road 85 in Dakota County, where a flashing LED stop sign was installed in October, 2008. (This site was included in the treatment group described in Chapter 2.) The county engineer indicated a problem with angle crashes at this intersection, where crash-involved drivers appeared to fail to stop at the existing stop sign, as opposed to stopping and then selecting an inadequate gap in the major road traffic stream. Table 4.1 shows data, taken from HSIS, for this intersection.

Table 4.1 Data for the Intersection of 160th St E and Dakota County Road 85

Year	Angle Crashes	Major Entering ADT	Minor Entering ADT	Major Speed Limit	Minor Speed Limit	Predicted Angle Crashes
2002	1	4350	1225	55	55	0.298
2003	0	4350	1225	55	55	0.298
2004	3	5550	1262.5	55	55	0.336
2005	1	6250	1300	55	55	0.363
2006	0	6650	1387.5	55	55	0.398
2007	4	7050	1475	55	55	0.435

We will show how the spreadsheet tool uses the data in Table 4.1 to answer questions (1) and (2) above.

4.2 Identifying Intersections with Atypical Crash Frequencies.

The starting point is equation (2.3) from Chapter 2, a simplified version of which is given below

$$\mu_t = \mu_0 \overline{\mu}_t \qquad (4.1)$$

As before, μ_t denotes the expected number of right-angle crashes at the intersection in question, during year t, and $\overline{\mu}_t = \exp(\beta_0 + \beta_1 X_{t,1} + \ldots + \beta_5 X_{t,5})$ describes how the expected frequency of angle crashes typically varies with respect to traffic volumes, speed limits, and type of intersection (four-legged vs T). Estimation of the coefficients $\beta_0,\ldots,\beta_5$ was described in Chapter 2, and a summary of the estimates used by the spreadsheet tool is given in Table 2.4.

Applying the estimates summarized in Table 2.4 to the data in Table 4.1 gives predicted frequencies of angle crashes at the intersection of 160th St. and County Road 85, for each year

2002-2007, and these are listed in the rightmost column of Table 4.1. Summing these predicted frequencies tells us that a typical 4-legged intersection with traffic volumes and speed limits similar to that at 160th St and County Road 85 is expected have about 2.13 angle crashes between 2002 and 2007. The observed crash frequency during this period was nine angle crashes, which suggests that angle crashes are happening more frequently than appears to be typical.

The other term on the right-hand side of equation (4.1), μ_0, is a multiplier, specific to each intersection, that captures the effect of unobserved, intersection-specific features affected the occurrence of angle crashes.

$\mu_0 = 1.0$, the intersection has a typical frequency of angle crashes,

$\mu_0 > 1.0$, the intersection has more angle crashes than is typical,

$\mu_0 < 1.0$, the intersection has fewer angle crashes than is typical.

As part of the before/after analysis described in Chapter 2 values for μ_0 were estimated for each reference and treatment site, and the first component of the spreadsheet tool computes a similar estimate for the intersection in question, using data such as that shown in Table 4.1.

Table 4.2 shows the first component of the spreadsheet tool where an estimate of the multiplier μ_0 has been computed for the intersection of 160th St and County Road 85.

Entering major and minor approach ADTs are entered by the user, together with

Major limit = 1, if major approach speed limit ≥ 55 mph
0, otherwise

Minor limit =1, if minor approach speed limit ≥ 55 mph,
0, otherwise

4-legged = 1, if intersection is four-legged
0, if intersection is T.

Table 4.2 Component of Spreadsheet Tool for Estimating if a Given Intersection Has an Atypical Frequency of Right-Angle Crashes

Major:	160th E		Minor:	CR 85	County: Dakota
nyear=	6		First Year=	2002	
Majoradt	**Minoradt**	**Majorlimit**	**Minorlimit**	**4-legged**	**Crashes**
4350	1225	1	1	1	1
4350	1225	1	1	1	0
5550	1262.5	1	1	1	3
6250	1300	1	1	1	1
6650	1387.5	1	1	1	0
7050	1475	1	1	1	4

High-hazard analysis

E[mu0]	3.572246
SD(mu0)	1.360616
p(mu0>1)	0.998

The spreadsheet then uses a Visual Basic for Applications (VBA) macro to compute the three quantities listed under the heading "High-hazard analysis" which reflect the estimate of μ_0 for the specific site:

E[mu0] = expected value of μ_0, given the site-specific data,

SD(mu0) = standard deviation of μ_0, given the site-specific data,

p(mu0>1) = probability $\mu_0 > 1.0$, given the site-specific data.

In order to allow for the uncertainty in the estimates of the prediction model parameters, the VBA macro includes a Monte Carlo sample of the parameter estimates, of length 5000. For each member of the Monte Carlo sample the macro computes the typical crash frequency for the intersection, generating a Monte Carlo outcome for μ_0. After doing this for all 5000 members, the macro computes summary statistics from the Monte Carlo sample of μ_0. For the intersection of 160th St. and County Road 84, E[mu0] = 3.57, indicating that angle crashes are about three-times for frequent at this intersection than would be expected if the intersection were typical. SD(mu0) = 1.36 indicates that there is a fair degree of uncertainty regarding the actual value of this intersection's μ_0, but p(mu0>1) = 0.998 indicates that with very high probability, this intersection has an atypically high frequency of angle crashes.

4.3 Predicting Flashing LED Stop Sign Crash Reduction

Suppose it has been determined that an intersection is a plausible candidate for installing a flashing LED stop sign. Whether or not a flashing LED stop sign is justified will depend on whether the benefits associated with the sign outweigh its costs, and assessing this will require a prediction of the crash reduction expected from installing the sign. The second component of the spreadsheet tools make this type of prediction, using the estimate, and associated uncertainty, of the safety effectiveness (crash reduction) found in Chapter 2. In essence, the predicted reduction for year t is found by multiplying the expected crash frequency for year t by the safety effectiveness (SE)

$$Expected\ reduction = \mu_t(SE) = \mu_0 \overline{\mu}_t(SE) \qquad (4.2)$$

As with the first component, a Monte Carlo sample of the coefficients $\beta_0,\ldots,\beta_5$ and other model parameters is used to allow for uncertainty in estimates, and Table 4.3 shows the component of the spreadsheet tool that accomplishes this.

This example shows a prediction over a 10 year time horizon (Future = 10), and where it is expected that no growth will occur in traffic volumes (ADT growth =0%). The user also entered the major and minor approach entering ADT for the first year of the forecast, along with characterizations of the intersection's speed limit and type, similar to that described in section 4.2. The spreadsheet's macro then uses a Monte Carlo sample to compute the expected number of crashes, and the associated standard deviation, for each year of the forecast horizon, on the assumption that flashing LED stop sign is not installed. The macro also computes the expected number of crashes prevented, and associated standard deviation, for each year of the time horizon, on the assumption that flashing LED stop signs are installed. In Table 4.3, for the base year we have entered a major approach ADT = 6600 vehicles, and minor approach ADT = 1575 vehicles, have indicated that the major and minor approach speed limits are at least 55 mph, and that the intersection is four-legged. The spreadsheet macro has then computed that, during the base year, we would expect 1.6 right angle crashes if the flashing LED stop sign is not installed, and a crash reduction of about 0.69 crashes if the flashing LED stop sign is installed. Since the assumed ADT growth rate is 0%, these predictions are the same for each year in the time horizon. The total expected crash reduction for the time horizon can be found be summing over

all years, in this case the tool predicts that about 6.9 angle crashes would be prevented over 10 years. This prediction could then be used as an input into a cost-benefit or cost-effectiveness analysis.

Table 4.3 Spreadsheet Component for Predicting Crash Reduction Effects of Flashing LED Stop Signs

			Future=	10	**ADT growth=**	0	%			
Base	**Major adt**	**Minor adt**	**Major limit**	**Minor limit**	**4-legged**		**E[crash]**	**SD[crash]**	**E[reduc]**	**SD[reduc]**
Values=	6600	1575	1	1	1		1.602114	0.537199	0.668597	0.388002
	6600	1575	1	1	1		1.602114	0.537199	0.668597	0.388002
	6600	1575	1	1	1		1.602114	0.537199	0.668597	0.388002
	6600	1575	1	1	1		1.602114	0.537199	0.668597	0.388002
	6600	1575	1	1	1		1.602114	0.537199	0.668597	0.388002
	6600	1575	1	1	1		1.602114	0.537199	0.668597	0.388002
	6600	1575	1	1	1		1.602114	0.537199	0.668597	0.388002
	6600	1575	1	1	1		1.602114	0.537199	0.668597	0.388002
	6600	1575	1	1	1		1.602114	0.537199	0.668597	0.388002
	6600	1575	1	1	1		1.602114	0.537199	0.668597	0.388002

Chapter 5
Summary and Conclusion

5.1 Summary

This project conducted a two-pronged investigation of the safety-related effects of flashing LED stop signs: a statistical study to estimate the crash reduction effect following installation of flashing LED stop signs and a field study looking at changes in the behavior of drivers approaching a stop-controlled intersection, before and after installation of a flashing LED stop sign.

Using a hierarchical Bayes before/after design, the statistical study compared the crash frequency after installation of a flashing LED stop signs at 15 intersections to a prediction of what that crash frequency would have been had the flashing LED stop signs not been installed. All intersections were through-stop controlled with undivided major roads, and the target crash type was right-angle crashes involving major approach and minor approach vehicles. The estimated reduction was about 41.5%, but with 95% confidence this reduction could be anywhere between 0% and 70.8%. The conclusion was that installation of the flashing LED stop signs reduced the frequency of angle crashes but that the magnitude of this reduction was uncertain.

For the field study, during two, three-day periods in June and July 2012, portable video equipment was used to record vehicle approaches at a through-stop controlled intersection in Chisago county. The standard stop signs on the minor approaches were then replaced with flashing LED stop signs and Video data were collected for two, three-day period in September and November 2012. After installing the flashing LED stop sign, there appeared to be no change in the relative proportion of clear stops versus clear non-stops when minor approach drivers did not face opposing traffic, but that after installation of the flashing LED stop sign the relative proportion of clear stops increased for drivers who did encounter opposing traffic.

Finally, for each of the four field data collection periods a random sample of 30 minor approach vehicles was selected. Speeds for these vehicles, when about 500 feet from the intersection, and average deceleration rates over the final 500 feet were then estimated using trajectory-based methods. Average approach speeds tended to be highest in June, somewhat lower in July, and lower yet in September and November, with September and November having roughly equal average speeds. The average deceleration rates showed a similar pattern.

5.2 Conclusions

The estimated reduction in angle crashes associated with installation of flashing LED stop signs was between about 0% and 71%, with a point estimate of about 41%, based on a treatment group of 15 intersections. The can be compared to the estimated reduction in angle crashes, following installation stop sign-mounted beacons, of 58.2% ± 32.6% (Srinivasan et al 2008, p. 22), based on a treatment group of seven intersections. Although qualified by the relatively small sample sizes and wide confidence intervals, a reasonable interpretation is that flashing LED stop signs appear to have an effect similar to that of stop sign-mounted beacons.

References

AASHTO (2010) *Highway Safety Manual*, American Association of Highway and Transportation Officials, Washington, DC.

Arnold, E., and Lantz, K. (2007) *Evaluation of Best Practices in Traffic Operations and Safety: Phase I: Flashing LED Stop Signs and Optical Speed Bars*, Virginia Transportation Research Council Report VTRC 07-R34, Virginia Transportation Research Council, Charlottesville, VA.

Aul, N., and Davis, G. (2006) "Use of propensity score matching method and hybrid Bayesian method to estimate crash modification factors of signal installation," *Transportation Research Record*, 1950, 17-23.

Christiansen, C., and Morris, C. (1997) "Hierarchical Poisson regression modeling," *Journal of the American Statistical Association*, 92, 618-632.

Davis, G. (2000a) "Accident reduction factors and causal inference in traffic safety studies: A review," *Accident Analysis and Prevention*, 32, 95-109.

Davis, G. (2000b) "Estimating traffic accident rates while accounting for traffic volume measurement error: A Gibbs sampling approach," *Transportation Research Record*, 1717, 94-101.

Davis, G. and Swenson, T. (2006) "Collective responsibility for freeway rear-ending accidents? An application of probabilistic causal models," *Accident Analysis and Prevention*, 38, 728-736.

Davis, G. and Yang, S. (2001) "Bayesian identification of high-risk intersections for older drivers via Gibbs sampling," *Transportation Research Record*, 1746,84-89.

Gates, T., Hawkins, H., Chrysler, S., Carlson, P., Holick, A., and Speigelman, C. (2003) *Traffic Operational Impacts of Higher-Conspicuity Sign Material*, Report FHWA/TX-04/4271-1, Federal Highway Administration, Washington, DC.

Hauer. E. (1997) *Observational Before-After Studies in Road Safety*, Elsevier Science, Oxford, UK.

Lunn, D., Thomas, A., Best, N., and Spiegelhalter, D. (2000) "WinBUGS-A Bayesian modeling framework: Concepts, Structure, and Extensibility," *Statistics and Computing*, 10, 325-337.

Murphy, B., and Hummer, J. (2007) "Development of crash reduction factors for overhead flashing beacons at rural intersections in North Carolina," *Transportation Research Record*, 2030, 15-21

Robbins, H. (1956) "An empirical Bayes approach to statistics," *Proceedings of the Third Berkeley Symposium on Mathematical Statistics and Probability*, Unversity of California Press, Berekley,CA, 157-163.

Srinivasan, R., Carter, D., Eccles, K., Persaud, B., Leffler, N., Lyon, C., and Amjadi, R. (2008) *Safety Evaluation of Flashing Beacons at STOP-Controlled Intersections*, Federal Highway Administration Report FHWA-HRT-08-044, Washington, DC.

Stackhouse, S., and Cassidy, P. *Warning Flashers at Rural Intersections*, Report to Minnesota Dept. of Transportation, St., Paul, MN, 1998.

Appendix A

Chapter 6 Intersections Used in Statistical Study Treatment Group

Intersections Used in Statistical Study Treatment Group

Intersection	County
MN-210 at U.S.169	Aitkin
Co Rd 24 at MN-23	Lyon
60th Ave S at U.S.75	Clay
110th Ave S at U.S.75	Clay
Co Hwy 2 at U.S.75	Clay
Co Hwy 18 at Co Hwy 11	Clay
Co Hwy 52 at 30th Ave S	Clay
160th St E at Co Rd 85	Dakota
Co Hwy 5 at Great River Rd	Aitkin
Co Hwy 10 at MN-200	Aitkin
Main St W at 4th Ave SW	Le Sueur
Co Rd 101 at MN-22	Le Sueur
Co Rd 5 at MN-111	Nicollet
Co Hwy 9 at MN-60	Jackson
Co Hwy 1 at MN-60	Cottonwood

Appendix B

Chapter 7 WinBUGS Model and Data for Statistical Study

WinBUGS Model and Data for Statistical Study

```
model
# individual deviations parameterized as multipliers with gamma(r,r) priors
# angle crashes as DV
# internally computed log adt variables
# no individual site CMFs
# 2011 and 2012 data added to treatment sites
# Hui's model 3
{
# compute Bayes estimates of GLM parameters and individual intersection deviations
for (i in 1:Nrow) {
logmajadt[i]<-log(X[i,1])
logminadt[i]<-log(X[i,2])
majadt[i]<-logmajadt[i]-mean(logmajadt[])
minadt[i] <- logminadt[i]-mean(logminadt[])
majlim[i]<-step(X[i,3]-54)
minlim[i]<-step(X[i,4]-54)
four_leg[i]<-X[i,5]
skewed0[i]<-X[i,6]
skewed1[i]<-X[i,7]
skewed2[i]<-X[i,8]
beacon[i]<-X[i,9]
year[i]<-Year[i]
muhat[i] <- exp(beta0+beta[1]*majadt[i]+beta[2]*minadt[i]+beta[3]*majlim[i]+beta[4]*minlim[i]+beta[5]*four_leg[i])
mu[i] <- mu0[Site[i]]*muhat[i]
Y1[i] ~ dpois(mu[i])
}

# compute simulated after signalization accident counts, along with before/after estimate of reduction factor
for (i in 1:Nafter) {
alogmajadt[i]<-log(Xa[i,1])
alogminadt[i] <- log(Xa[i,2])
amajlim[i]<-step(Xa[i,3]-54)
aminlim[i]<-step(Xa[i,4]-54)
amajadt[i]<-alogmajadt[i]-mean(logmajadt[])
aminadt[i]<-alogminadt[i]-mean(logminadt[])
afour_leg[i]<-Xa[i,5]
askewed0[i]<-Xa[i,6]
askewed1[i]<-Xa[i,7]
askewed2[i]<-Xa[i,8]
abeacon[i]<-Xa[i,9]
ayear[i]<-Yeara[i]
muhata[i] <-  exp(beta0+beta[1]*amajadt[i]+beta[2]*aminadt[i]+beta[3]*amajlim[i]+beta[4]*aminlim[i]+beta[5]*afour_leg[i])
mua[i] <- mu0[Sitea[i]]*muhata[i] }

bpost<-b+sum(mua[])
apost <- a+sum(Ya1[])
theta ~dgamma(apost,bpost)
arf <- 1-theta
parf<- step(arf)

pbeta0<-step(beta0)
for (i in 1:Nbeta) {pbeta[i]<-step(beta[i])}

# Prior distributions
for (i in 1:Nsite) {mu0[i] ~ dgamma(r,r)}
for (i in 1:Nbeta) { beta[i]~ dnorm(0,1.0E-06) }
beta0~dnorm(0,1.0E-06)
rx ~dpar(1,1)
r <- rx-1
kdisp <- 1/r
}
```

Appendix C

Chapter 8 Visual Basic for Applications Macro Implementing Decision Tool

Visual Basic for Applications Macro Implementing Decision Tool

```
Function gamrand(alpha, beta)

' Generates gamma random numbers, alpha = shape parameter, 1/beta = scale parameter
' Uses Best's alorithm when alpha >0, and RGS otherwise
' see L. Devroye, Non-Uniform Random Number Generation, 1985, pp.410 & 426

Dim t, b, c, u, w, v, x, y, z As Double
Dim accept As Integer

If alpha <= 1# Then
  t = 0.07 + 0.75 * Sqr(1 - alpha)
  b = 1 + (alpha * Exp(-t)) / t
  c = 1 / alpha
  accept = 0
  Do While accept < 1
    u = Rnd
    w = Rnd
    v = b * u
    If v <= 1# Then
      x = t * (v ^ c)
      If (w <= (2 - x) / (2 + x)) Or (w <= Exp(-x)) Then
        accept = 2
      End If
    End If
   If v > 1 Then
     x = -Log(c * t * (b - v))
     y = x / t
     If ((w * (alpha + y - alpha * y)) <= 1#) Or (w <= y ^ (alpha - 1)) Then
       accept = 2
     End If
   End If
 Loop
 gamrand = x / beta
Else
 b = alpha - 1
 c = (12 * alpha - 3) / 4
 accept = 0
 Do While accept < 1
   u = Rnd
   v = Rnd
   w = u * (1 - u)
   y = (u - 0.5) * Sqr(c / w)
   x = b + y
   If x > 0 Then
```

```
      z = 64 * (v ^ 2) * (w ^ 3)
      If (z <= (1 - 2 * ((y ^ 2) / x))) Or (Log(z) <= 2 * ((b * Log(x / b)) - y)) Then
        accept = 2
      End If
    End If
  Loop
  gamrand = x / beta
End If

End Function

Sub highhazard()

Dim beta0(1 To 5000) As Double
Dim beta1(1 To 5000) As Double
Dim beta2(1 To 5000) As Double
Dim beta3(1 To 5000) As Double
Dim beta4(1 To 5000) As Double
Dim beta5(1 To 5000) As Double
Dim arf(1 To 5000) As Double
Dim r(1 To 5000) As Double
Dim a(1 To 5000) As Double
Dim b(1 To 5000) As Double
Dim mu0(1 To 5000) As Double
Dim musum(1 To 5000) As Double



Dim majoradt(1 To 10) As Double
Dim minoradt(1 To 10) As Double
Dim majorlim(1 To 10) As Integer
Dim minorlim(1 To 10) As Integer
Dim fourleg(1 To 10) As Integer
Dim y(1 To 10) As Integer

Dim bmajadt(1 To 20) As Double
Dim bminadt(1 To 20) As Double
Dim bmajlim(1 To 20) As Integer
Dim bminlim(1 To 20) As Integer
Dim b4leg(1 To 20) As Integer

Dim growrate, mupbar, mup, artemp, mubar, musig, exredbar, exredsig As Double


Dim nmc, nyearin, nyearout, offset, ysum, i, j As Integer
Dim logmajadt, logminadt, mu0bar, mu0sig, mu0p As Double
```

```
'Read size of MCMC sample and ADT shift from Worksheet 2

nmc = Worksheets("Sheet2").Cells(2, 13).Value
logmajadt = Worksheets("Sheet2").Cells(2, 11).Value
logminadt = Worksheets("Sheet2").Cells(2, 12).Value

' Read MCMC posteriors for GLM coefficients (betax), accident reduction factor (arf),
' random effects parameter (r) from Worksheet 2

For i = 1 To nmc
  beta0(i) = Worksheets("Sheet2").Cells(1 + i, 1).Value
  beta1(i) = Worksheets("Sheet2").Cells(1 + i, 2).Value
  beta2(i) = Worksheets("Sheet2").Cells(1 + i, 3).Value
  beta3(i) = Worksheets("Sheet2").Cells(1 + i, 4).Value
  beta4(i) = Worksheets("Sheet2").Cells(1 + i, 5).Value
  beta5(i) = Worksheets("Sheet2").Cells(1 + i, 6).Value
  arf(i) = Worksheets("Sheet2").Cells(1 + i, 7).Value
  r(i) = Worksheets("Sheet2").Cells(1 + i, 8).Value
Next i

offset = 4
ysum = 0

' Read historical data for site of interest from Worksheet 1

nyearin = Worksheets("Sheet1").Cells(offset + 1, 2).Value

For i = 1 To nyearin
  majoradt(i) = Worksheets("Sheet1").Cells(offset + 4 + i, 1).Value
  minoradt(i) = Worksheets("Sheet1").Cells(offset + 4 + i, 2).Value
  majorlim(i) = Worksheets("Sheet1").Cells(offset + 4 + i, 3).Value
  minorlim(i) = Worksheets("Sheet1").Cells(offset + 4 + i, 4).Value
  fourleg(i) = Worksheets("Sheet1").Cells(offset + 4 + i, 5).Value
  y(i) = Worksheets("Sheet1").Cells(offset + 4 + i, 6).Value
  ysum = ysum + y(i)
Next i

For i = 1 To nmc
  musum(i) = 0
  For j = 1 To nyearin
    musum(i) = musum(i) + Exp(beta0(i) + beta1(i) * (Log(majoradt(j)) - logmajadt) +
beta2(i) * (Log(minoradt(j)) - logminadt) + beta3(i) * majorlim(j) + beta4(i) *
minorlim(j) + beta5(i) * fourleg(j))
  Next j
  a(i) = r(i) + ysum
```

```
  b(i) = r(i) + musum(i)
  mu0(i) = gamrand(a(i), b(i))
  mu0bar = mu0bar + mu0(i)
  mu0sig = mu0sig + mu0(i) * mu0(i)
  If mu0(i) > 1 Then
     mu0p = mu0p + 1
  End If
Next i

mu0bar = mu0bar / nmc
mu0p = mu0p / nmc
mu0sig = Sqr((mu0sig / nmc) - mu0bar * mu0bar)

' Write mean, standard deviation and probability of mu0 to Worksheet 1

Worksheets("Sheet1").Cells(offset + 14 + 1, 2).Value = mu0bar
Worksheets("Sheet1").Cells(offset + 14 + 2, 2).Value = mu0sig
Worksheets("Sheet1").Cells(offset + 14 + 3, 2).Value = mu0p

' Read desired number of years for reduction prediction

nyearout = Worksheets("Sheet1").Cells(offset + 1, 12).Value

' Compute predictions if desired number of years greater than 0

If nyearout > 0 Then

' Read growth rate
  growrate = Worksheets("Sheet1").Cells(offset + 1, 14).Value

' Read base values for GLM independent variables
  bmajadt(1) = Worksheets("Sheet1").Cells(offset + 5, 9).Value
  bminadt(1) = Worksheets("Sheet1").Cells(offset + 5, 10).Value
  bmajlim(1) = Worksheets("Sheet1").Cells(offset + 5, 11).Value
  bminlim(1) = Worksheets("Sheet1").Cells(offset + 5, 12).Value
  b4leg(1) = Worksheets("Sheet1").Cells(offset + 5, 13).Value

' Compute growth factor
  growfac = (1 + (growrate / 100))

'Compute indepdendent variable values for each year in forecast horizon
For i = 2 To nyearout
  bmajadt(i) = bmajadt(i - 1) * growfac
  bminadt(i) = bminadt(i - 1) * growfac
  bmajlim(i) = bmajlim(i - 1)
  bminlim(i) = bminlim(i - 1)
```

```
  b4leg(i) = b4leg(i - 1)
Next i

'Compute expected number of crash, and expected crash reduction, for each year of
forecast horizon
' togehter with their standard deviations

For j = 1 To nyearout
  mubar = 0
  musig = 0
  exredbar = 0
  exredsig = 0
  For i = 1 To nmc
    mupbar = Exp(beta0(i) + beta1(i) * (Log(bmajadt(j)) - logmajadt) + beta2(i) *
(Log(bminadt(j)) - logminadt) + beta3(i) * bmajlim(j) + beta4(i) * bminlim(j) + beta5(i) *
b4leg(j))
    mup = mupbar * mu0(i)
    artemp = mup * arf(i)
    mubar = mubar + mup
    musig = musig + (mup * mup)
    exredbar = exredbar + artemp
    exredsig = exredsig + (artemp * artemp)
  Next i
  mubar = mubar / nmc
  musig = Sqr((musig / nmc) - mubar * mubar)
  exredbar = exredbar / nmc
  exredsig = Sqr((exredsig / nmc) - exredbar * exredbar)
  Worksheets("Sheet1").Cells(offset + 4 + j, 9).Value = bmajadt(j)
  Worksheets("Sheet1").Cells(offset + 4 + j, 10).Value = bminadt(j)
  Worksheets("Sheet1").Cells(offset + 4 + j, 11).Value = bmajlim(j)
  Worksheets("Sheet1").Cells(offset + 4 + j, 12).Value = bminlim(j)
  Worksheets("Sheet1").Cells(offset + 4 + j, 13).Value = b4leg(j)
  Worksheets("sheet1").Cells(offset + 4 + j, 15).Value = mubar
  Worksheets("Sheet1").Cells(offset + 4 + j, 16).Value = musig
  Worksheets("Sheet1").Cells(offset + 4 + j, 17).Value = exredbar
  Worksheets("Sheet1").Cells(offset + 4 + j, 18).Value = exredsig
Next j

End If
End Sub
```